

Feasibility of bolted connectors in hybrid FRP-steel structures

Olivier, Gerhard; Csillag, Fruzsina; Christoforidou, Angeliki; Tromp, Liesbeth; Veltkamp, Martijn; Pavlovic, Marko

DOI

[10.1016/j.conbuildmat.2023.131100](https://doi.org/10.1016/j.conbuildmat.2023.131100)

Publication date

2023

Document Version

Final published version

Published in

Construction and Building Materials

Citation (APA)

Olivier, G., Csillag, F., Christoforidou, A., Tromp, L., Veltkamp, M., & Pavlovic, M. (2023). Feasibility of bolted connectors in hybrid FRP-steel structures. *Construction and Building Materials*, 383, Article 131100. <https://doi.org/10.1016/j.conbuildmat.2023.131100>

Important note

To cite this publication, please use the final published version (if applicable).
Please check the document version above.

Copyright

Other than for strictly personal use, it is not permitted to download, forward or distribute the text or part of it, without the consent of the author(s) and/or copyright holder(s), unless the work is under an open content license such as Creative Commons.

Takedown policy

Please contact us and provide details if you believe this document breaches copyrights.
We will remove access to the work immediately and investigate your claim.



Feasibility of bolted connectors in hybrid FRP-steel structures

Gerhard Olivier^a, Fruzsina Csillag^b, Angeliki Christoforidou^a, Liesbeth Tromp^c,
Martijn Veltkamp^d, Marko Pavlovic^{a,*}

^a TU Delft Steel and Composite Structures Delft, the Netherlands

^b Arup Infrastructure Amsterdam, the Netherlands

^c Royal HaskoningDHV Infrastructure Rotterdam, the Netherlands

^d FiberCore Europe, the Netherlands

ARTICLE INFO

Keywords:

Bolted connections
Slip-resistant connections
Fatigue performance
Combined short- and long-term loading
Injected steel reinforced resin

ABSTRACT

Due to the low weight and excellent durability of composite materials, Fibre Reinforced Polymer (FRP) decks mounted on steel superstructures are becoming increasingly common in engineering practice. Bolted joints are generally used to facilitate connections between an FRP deck and steel girders in road bridges. The connections are subjected to both high magnitude static forces as well as fatigue loading due to overpassing vehicles. With ever increasing traffic on both road and railway bridges, fatigue performance is of critical concern. Bolted FRP joints have been extensively researched in the past under static loading, but less is known about the fatigue and creep behaviour of such joints. Furthermore, little research exists on non-pultruded FRP profiles connected using bolted connections. Therefore, the objective of this research is to investigate connectors' feasibility by means of static, fatigue and creep experiments on four different types of bolted joints comprising mechanical connectors and injection techniques. The study focuses on application in vacuum infused GFRP panels with integrated webs made of multi-directional laminates connected to steel bridge superstructures. In addition, experimental results are used to validate Finite Element Analyses (FEA). Based on the obtained results, the novel injected steel-reinforced resin (ISRR) connector shows promising potential in hybrid steel-FRP bridges where good fatigue endurance of the connection, are required.

1. Introduction

By utilising benefits from both materials, steel-FRP hybrid structures are a promising candidate in bridge renovation projects where the original deck (steel, concrete or timber) has been deteriorated whilst the main (e.g., steel girders) load carrying structure is unaffected. Due to high strength-to-weight ratio, FRP decks impose minimum additional weight on the existing structure. Low weight also enables prefabrication and installation of large deck segments leading to minimum traffic hindrance, which is of significant benefit in bridge infrastructure renovation projects. To implement successful steel to FRP projects, adequate structural performance of the deck-to-girder connection is required. To visualise this scenario, Fig. 1 depicts an FRP deck placed upon steel main load carrying structure of a bascule type movable bridge. In case that hybrid interaction between the FRP deck and the girder is engaged, a slip-resistant connection is required to obtain reliable shear interaction and sufficient fatigue endurance in a bridge application. In addition, the

pull-out resistance of the connectors may play important role as the tensile forces can arise at the connection to flanges of steel girders neighbouring the local wheel loads.

Extensive research on adhesive [1] and grouted shear stud connection [2] between the steel and FRP have been performed. In comparison, due to localised load transfer, bolted connections have been examined to a lesser extent. Bolted connections promote demountability and material reuse of the steel girders and FRP, thereby promoting circular economy. Ordinary and blind bolted connections in double lap joint (DLJ) configurations with GFRP pultruded plates were tested by Zafari et al. [3]. Static and fatigue loading was applied and in both loading conditions the performance of the ordinary bolts was superior. These connections were also tested at elevated temperatures [4]. Additionally, static and fatigue tests were then done to evaluate the performance of multi-bolted DLJ with stainless steel, basalt FRP and hybrid steel-FRP bolts which were the ones that showed the most promising results [5]. Another comparative study between different types of bolted connections was performed

* Corresponding author.

E-mail address: m.pavlovic@tudelft.nl (M. Pavlovic).

<https://doi.org/10.1016/j.conbuildmat.2023.131100>

Received 13 March 2022; Received in revised form 4 September 2022; Accepted 17 March 2023

Available online 13 April 2023

0950-0618/© 2023 The Author(s). Published by Elsevier Ltd. This is an open access article under the CC BY license (<http://creativecommons.org/licenses/by/4.0/>).

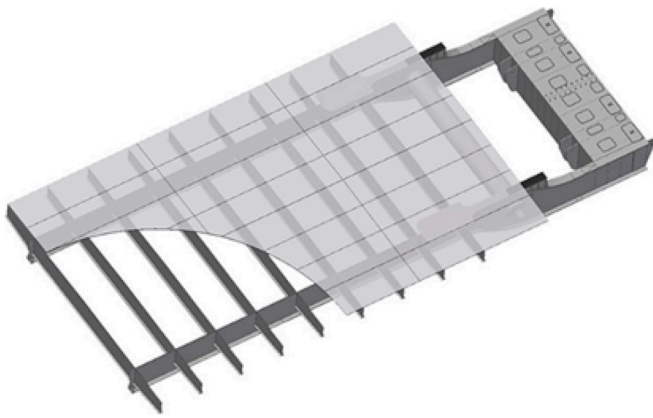
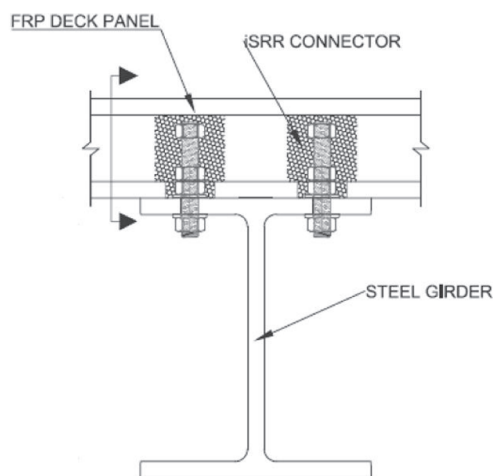


Fig. 1. Example of an FRP Deck on a movable bridge.

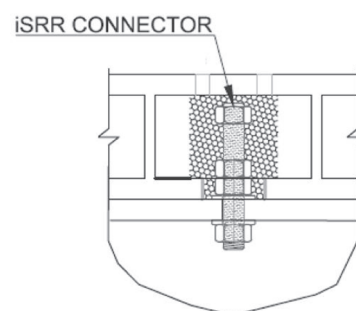
by Van Wingerde et al. [6]. The fatigue performance of ordinary bolts was compared with that of injected bolts with the latter resulting in a significantly improved performance when tested under fully reversed cycles of loading. Standard and injected bolts were also compared by Zafari et al. [3], where cyclic tests were conducted in DLJ and single lap joint (SLJ) configurations and was concluded that the injection bolts can be a promising solution for applications with slip and fatigue resistant requirements.

In the effort of making the injection materials cheaper, stiffer and creep resistant, steel shots are applied as a reinforcement of the conventional resin systems. This material, comprising of steel shot and a polymeric resin is called Steel Reinforced Resin (SRR) and was initially investigated as an alternative injection material for injection bolts [7]. This type of connection was explored as an alternative way to connect concrete beams to steel plates with a broader view to be applied in composite floor systems [8].

Apart from applying SRR material in injection bolts, there has been research that proves that SRR material can form a connector between FRP material and steel [9,10]. This novel type of connection seems to be very favorable when it comes to bridge renovation or even new projects that qualify the use of composites for the upper part of the deck of a bridge. More specifically, the SRR material surrounds a standard bolt and fills the gap that exists between the bolt and facing of the FRP. This type of connection is called injected SRR (iSRR) connector and is illustrated in Fig. 2.



a) Transverse section of beam



b) Longitudinal section of the beam

Fig. 2. Isrr connector between frp sandwich panel and steel girder.

In this paper, apart from the iSRR connector, blind bolts and injection bolts are also considered as a solution for connecting FRP decks to the steel girders. All of these studies [9–12] cover the understanding and characterisation of shear and tensile behaviour of those connectors. The aim is to improve the design life prediction of the connector performance through experimental testing and detailed Finite Element Analysis (FEA). The experimental specimens are designed in such a way as to obtain realistic failure modes as compared to those that would be obtained at the connections between an FRP deck and steel girders in bridges. Finite element models go to deep level of geometrical details at joint level and include damage material models of FRP and steel. Based on the experimental campaign, as well as FEA models, connector behaviour is quantified and application fields are identified. The objective of this paper is to compare the available experimental and numerical results available in the literature [9,10] related to steel to FRP connections for highway bridges. In addition to providing a holistic context of the existing knowledge, this paper presents novel experimental results on axial resistance, fatigue behaviour and a numerical sensitivity study related to boundary conditions to replicate true behaviour of steel reinforced connectors in a structure.

2. Connector types and experimental approach

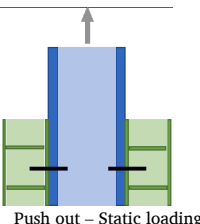




The study presented here focuses on four types of bolted connectors used in deck-to-girder connections. Experiments are conducted to investigate the long- and short-term connector performance. A clear distinction will be made between the short-term loading experiments performed by Csillag (2018) [13] as well as a more recent experimental research campaign to quantify the long term-connector performance. The investigated connectors include: two blind bolts (namely Ajax and Lindapter connectors) as well as two slip-resistant connector types (conventional epoxy injected bolts as well as the iSRR connector). An overview of all the experimental and numerical works reported in this paper is presented in Table 1.

The iSRR connector is a novel, hybrid joining technology developed byCsillag [10]. In this experimental campaign the iSRR connector is installed as depicted in Fig. 2, whereby a rod (or bolts connected by means of a coupler) is clamped to the top flange of a steel girder and embedded within a large cylindrical cut-out within the FRP deck which houses the steel reinforced resin injection piece (for more detailed information see [9]).

In the **short-term loading experiments**, Ajax, Lindapter and the iSRR connector are investigated. All examined connectors are of 20 mm

Table 1

Overview of experimental and numerical work reported in this study.

Type of experiment ¹	Type of connector			
	Ajax	Lindapter	iSRR	Injected
	Tested & FEM	Tested & FEM	Tested & FEM	N/A
	Tested	Tested	Tested	N/A
	N/A	Tested & FEM	Tested & FEM	Tested & FEM
	N/A	Tested	Tested	Tested
	N/A	N/A	FEM	N/A

1: Green colour for FRP, blue colour for steel, black colour indicates the connector, arrow denotes the loading direction.

nominal diameter. The key feature of Ajax and Lindapter connectors is the possibility to be installed from one side from below the FRP deck via predrilled holes by means of a foldable washer and expandable sleeve, respectively. In all experiments, connectors are installed in GFRP deck panels with integrated webs and facings made of multi-directional laminates, produced by FiberCore Europe by the vacuum infusion process (fibre volume fraction 54%). The facings of the FRP panels contain the following E-glass fibre composition: $[0^\circ/75\%; 90^\circ/8.4\%/\pm 45^\circ/16.6\%]$ and a matrix comprising of polyester resin.

In the push-out experiments, the FRP deck panels were connected with the 3 different types of bolted connectors to an HEB260B Grade S355 profile as shown in Fig. 3. The principle fibre direction in the facings was perpendicular to the orientation of steel beam. In total 8 push-out tests were performed, 2 of the Ajax and 3–3 of the Lindapter and iSRR connector. The static loading was exerted on the top of the HEB profile by a hydraulic jack. In total 6 LVDTs (Linear Variable Displacement Transducer) were installed on the specimens: 4 LVDTs were attached next to the bolts measuring the slip between the steel beam and the FRP deck, and 2 perpendicular to the load direction on the front side of the specimen to measure separation of the panels from the steel beam. The loading regime started with 25 cycles at an estimated 40% level of the ultimate load followed by the gradually increasing loading till failure. The jacking load and the average slip measured by the 4 vertical LVDTs were used to construct the load-slip curves of the push-out experiments, which are the main source for characterisation of the connector performance in shear.

All in all, 9 pull-out experiments (i.e. 3 specimens per bolt type) were conducted on the Ajax, Lindapter and the iSRR connectors during the short-term loading experimental campaign to assess their tensile performance [14]. In these tests, 500×500 mm square shape deck panels

with a central bolt were connected to a stiff steel frame to exert tensile load on the connection as is shown in Fig. 4. The sandwich panels were hold down by 40 mm thick, load-distributor steel plates and a hollow section profile. As a result of this test set-up, centric tensile force was applied on the bolted connection by the hydraulic jack, pulling the bolt upward. The tensile force and displacement of the jack was recorded to construct force displacement curves of the specimens.

In the **long-term loading experiments**, two commercially applied connectors (namely epoxy injected bolts and Lindapter connectors), as well as a modified version of the aforementioned iSRR connector were investigated. The conventional injected bolts, as used in steel structures, utilise epoxy resin (Araldite) and are placed in oversized holes. To simplify experimentation, single lap joint (SLJ) specimens were prepared containing a single FRP plate (representing the bottom facing of an FRP deck panel) connected to steel plates (grade S355). This set-up, as depicted in Fig. 5, facilitates comparisons of connector performance and analysis of failure mechanisms. The Ajax connectors tested in the push-out and pull-out experiments were not investigated under long-term loading. This was based on the results of a preliminary testing campaign which found that the foldable washer of the Ajax connector failed prematurely under cyclic loading, thereby excluding it from use in applications that require a high fatigue endurance. A detailed comparison between the SLJ and original hybrid-beam set-up is presented in Section 6. The fibre composition of the FRP plates $[0^\circ/62.5\%; 90^\circ/12.5\%/\pm 45^\circ/25\%]$ was altered with respect to the aforementioned push-out experiments in order to comply to the recommendations of CUR 96 (2017) [15] regarding the minimum fibre volume (12.5%) in all directions.

Results from the short-term and long-term loading regimes are presented separately in the subsequent sections of this paper.

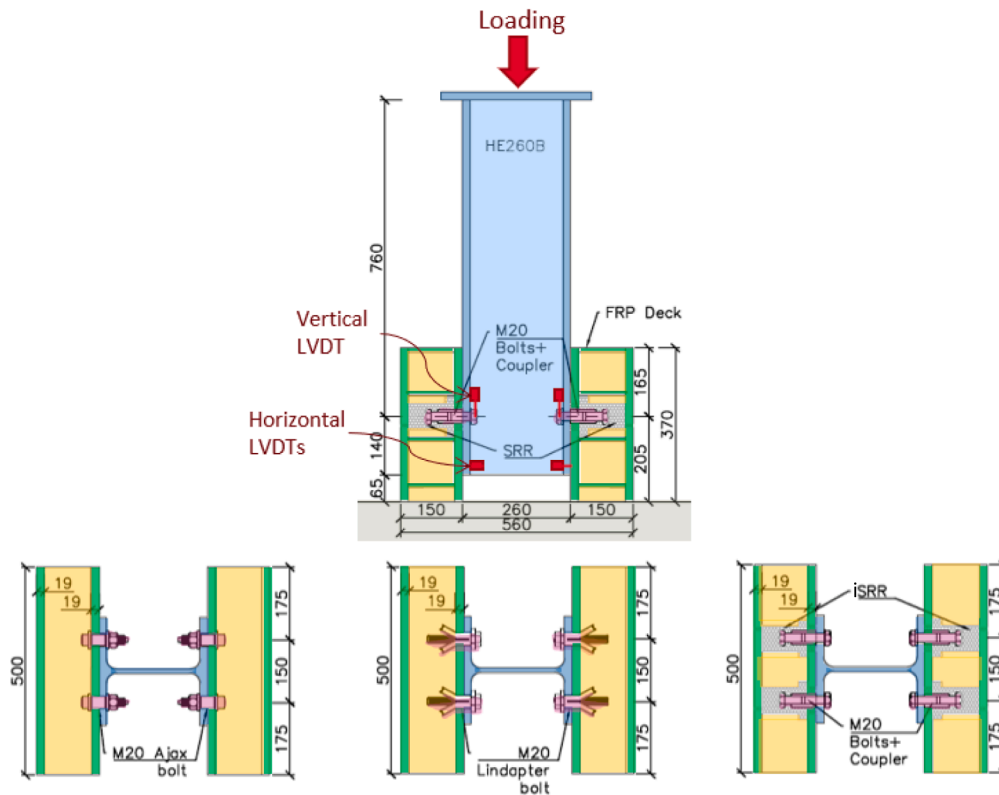


Fig. 3. Push-out experimental configuration (Csillag, 2021 [10]).

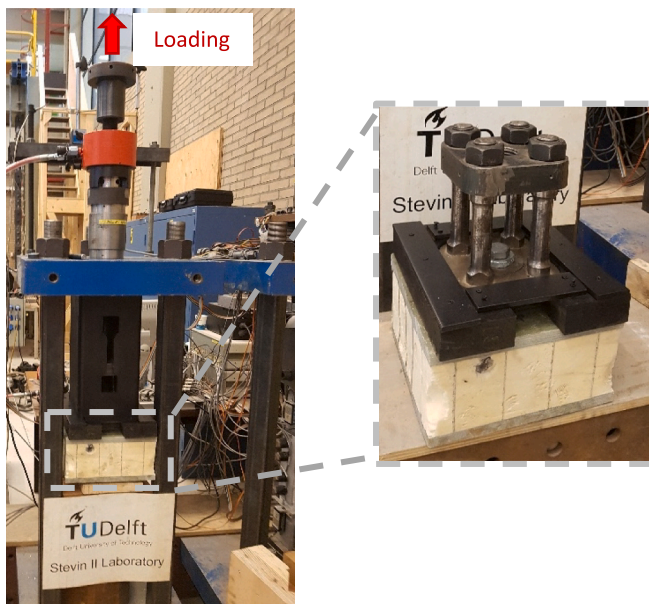


Fig. 4. Pull-out experimental configuration.

3. Short-term loading: shear and pull-out behaviour

3.1. Experiments

First the feasibility of commercially available blind-bolted vs. the novel iSRR connectors is examined in push-out tests by comparing their shear resistance in segments of GFRP deck panels, as shown in Fig. 6.

The figure depicts the experimentally obtained push-out failure modes of each connector.

FRP bearing failure, accompanied by excessive connector yielding, was observed in the specimens with M20 (grade 8.8) blind bolted connectors. Bolt yielding of the Ajax and Lindapter connectors was observed at average shear resistance per connector of approximately 200 kN and 150 kN, respectively (see Fig. 9). Although being demountable, Ajax shear connectors are impossible to mount again in a second life cycle. Due to extensive connector bending, Lindapter connectors also proved to be non-demountable.

When considering the iSRR connector, bolt shear failure governed ultimate resistance, occurring at approximately 25% lower force as compared to the blind-bolt connectors. The injected piece of the iSRR connector as well as FRP deck panel were undamaged, thereby enabling reuse of the panel in a second life cycle. The iSRR connector was found to possess limited ductility due to the occurrence of bolt shear failure at the FRP-Steel interface, as opposed to the quasi-ductile bearing failure and accompanied connector yielding observed in the blind bolted specimens. In second series of experiments, bolts of higher grade (10.9) were used for iSRR which resulted in expected improvement of the ductility allowing more than 6 mm of slip at failure (see Section 4).

In addition to the push out experiments, pull-out experiments were performed on bolted connection specimens using the same connector types. The typical failure mode and force-displacement curve per connector in the pull-out experiments is shown in Fig. 7 and Fig. 8.

Peak loads at the onset of non-linearity (i.e. first observation of FRP cracking and delamination) were measured on average at 58.7 kN, 42.6 kN and 69.3 kN in the Ajax, Lindapter and iSRR connected panels, respectively. Ultimate tensile resistances were measured on average as 95.7 kN; 61.3 kN and 88.4 kN in the Ajax, Lindapter and iSRR connected panels respectively. These results indicate the superior resistance of the iSRR connector to “first crack” as well as force recovery after

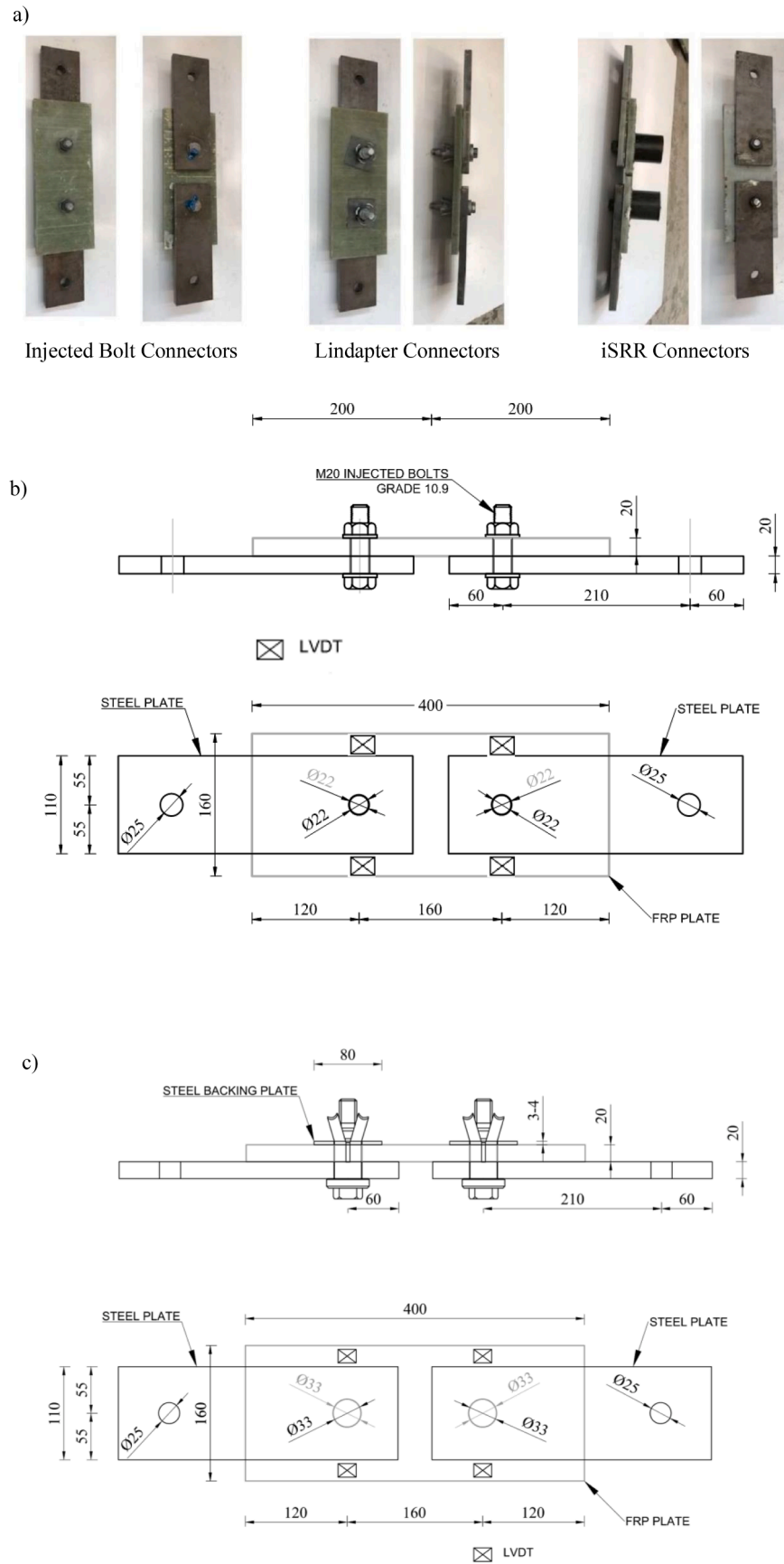


Fig. 5. Three types of shear connectors for FRP deck panels: specimens comprising of 2 connectors in single-lap shear joint (SLJ) configuration (dimensions in millimeters): a) prepared specimens, b) Injected Bolt connectors, c) Lindapter connectors and d) iSRR connectors.

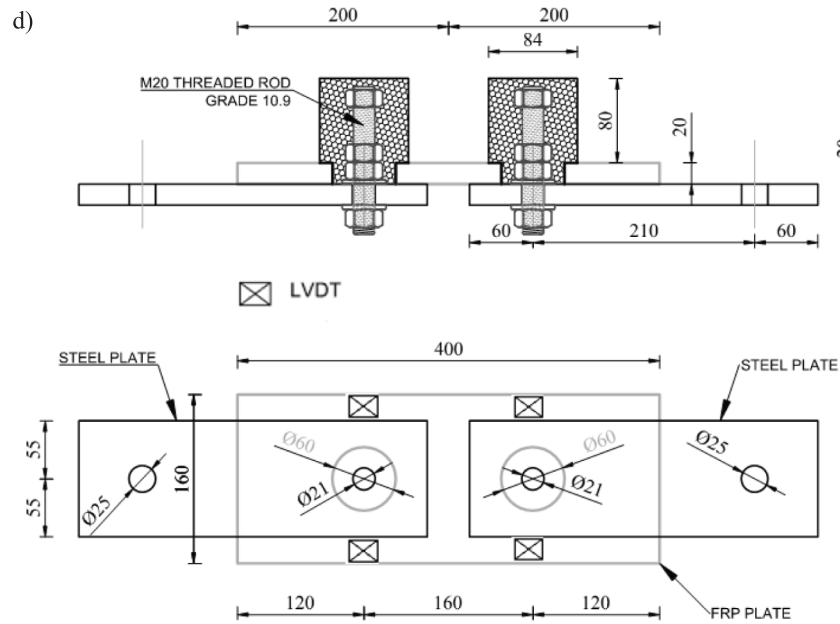
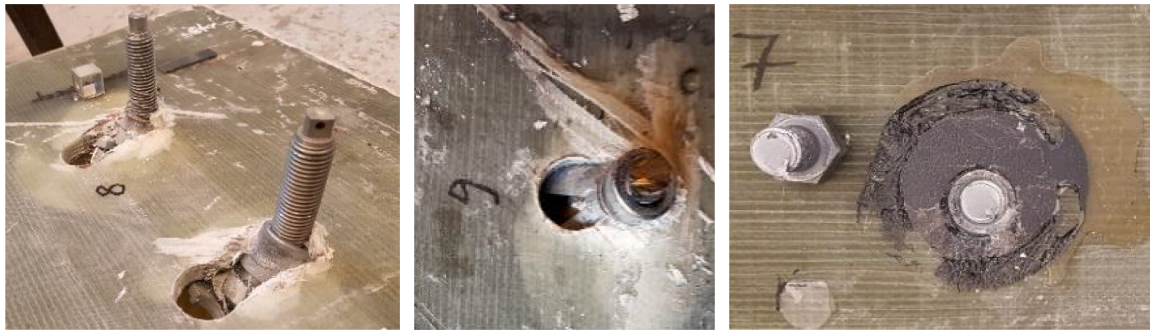


Fig. 5. (continued).



a) Ajax Bolts

b) Lindapter connector

c) iSRR connector

Fig. 6. Failure modes in push-out experiments of connectors in FRP deck panels [13].



a) Ajax Bolts

b) Lindapter connector

c) iSRR connector

Fig. 7. Failure modes in pull-out experiments of connectors in FRP deck panels [16].

delamination in the blind-bolted specimens.

With regards to the short-term loading experiments performed on the SLJ specimens, the following experimental methodology was adopted:

prior to the long-term loading experiments on the SLJ specimens, a set of monotonic static loading experiments were performed on the three connector types. The specimens tested were loaded until failure to

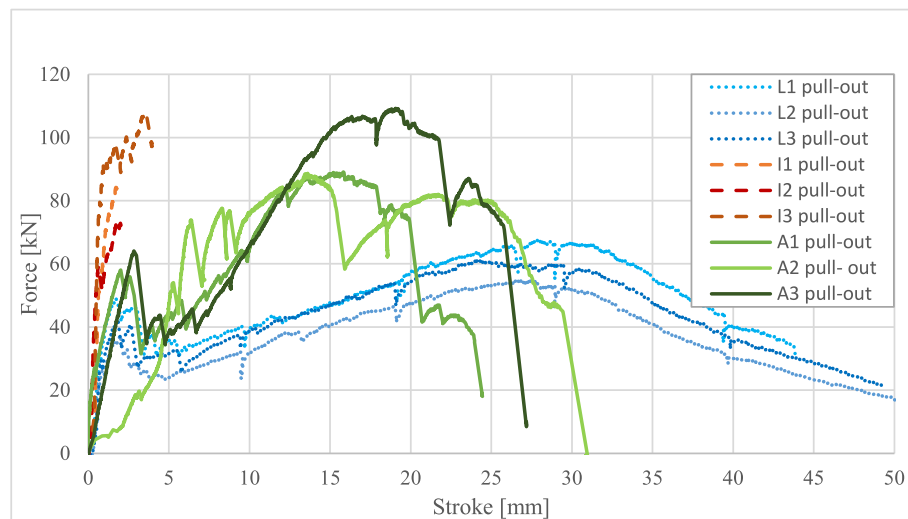


Fig. 8. Force-displacement curves of pull-out specimens [16] (L = Lindapter, I = iSRR, A = Ajax bolted connector).

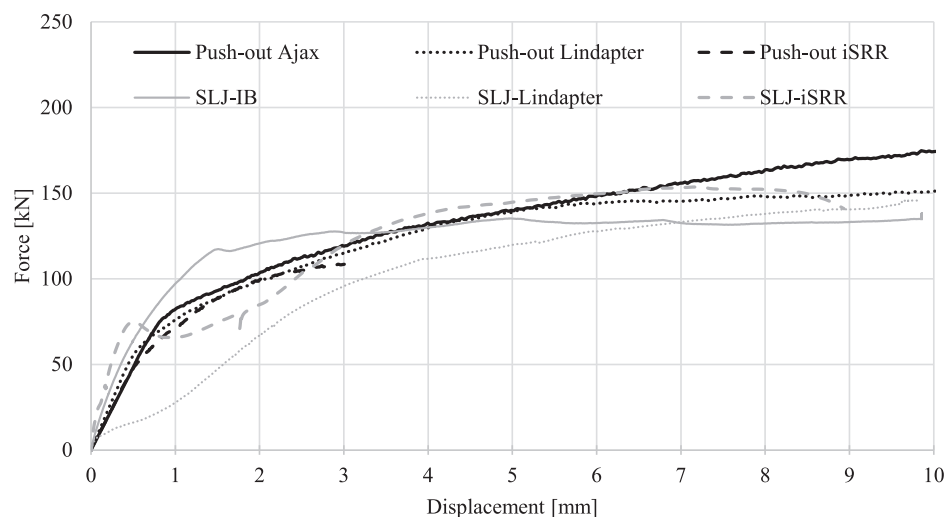


Fig. 9. Monotonic Static Loading Experimental Results: Applied force vs Connector Displacement.

obtain their shear resistance as well as load-slip behaviour including initial stiffness, initial slip and ultimate slip capacity. Individual connector force-slip behaviour was recorded by means of LVDTs. Static resistances ranging between 135 kN and 160 kN were obtained across the three specimen types.

The monotonic static loading experiments of both experimental campaigns are compared in Fig. 9. It is evident that, the previous limited ductility of the iSRR connector (as recorded in the push-out experiments) has been addressed. This is facilitated by the use of a higher strength grade of the metallic connector (10.9 vs 8.8), enabling an ultimate slip of approximately 8 mm, thereby classified as ductile according to EN1994-1-1 [17]. Larger initial stiffness of the iSRR connector in SLJ compared to Push-out set-up, approx. 200 kN/mm vs. 100 kN/mm, respectively, is due to full preloading of the M20 bolt in the former. Bolts were preloaded only within the steel plate, between the inner and outer nut, by means of a moment wrench to the force of approx. $F_{p,c} = 170$ kN. This also results in the plateau behaviour of the iSRR in SLJ set-up once the slip resistance of approx. 75 kN is reached corresponding to the apparent slip factor between the bolt and the steel plate of approx. 0.45. After the nominal hole clearance of 1 mm is void by the bolt slip in the hole, the bearing load transfer mechanism is attained resulting in increase of load in the connector with the

increasing displacement. The Lindapter connectors were not preloaded in either of the set-ups further than what was required to wedge the connection by activating the expandable sleeve, see details in Csillag and Pavlović [10]. Initial stiffness of the Lindapter is lower in the SLJ compared to Push-out set-up, since 25 cycles at an estimated 40% of the ultimate load were applied in the Push-Out set-up experiments, resulting in voiding the hole clearance before monotonic load application until failure. Full preloading of the Lindapter connectors is not feasible because the resin dominated creep effects through thickness of the composite plate would lead to preloading loss as the composite plate is part of the preloading package. Furthermore, trial preloading of the Lindapter connectors showed that application of more than 60 Nmm (corresponding to ~15 kN preload) torque resulted in cracking of the composite plate due to expansion of the hole by the inclined sleeve piece [3], see Fig. 15b and Fig. 18a illustrating such an effect.

The ultimate force and displacement per connector type in both experimental campaigns (Push-out and SLJ experiments) are summarised in Table 2.

Based on the aforementioned results, it can be seen that the feasibility of each connector type depends on its intended application as well as prevailing design criteria. This is illustrated by considering the advantages per connector type: shear resistance in terms of Ajax

Table 2

Averaged ultimate force and displacement per connector across experimental campaigns.

Connector	Push-out Ajax	Push-out Lindapter	Push-out iSRR	SLJ IB	SLJ Lindapter	SLJ iSRR
F_{ult} [kN]	207.4	164.3	123.0	143.5	153.8	153.9
(CoV)	(5.4)	(19.9)	(14.9)	(4.5)	(6.8)	(5.2)
δ_u [mm]	18.9	19.0	4.8	9.5	9.8	8.5

connectors, ease of installation of Lindapter and tensile resistance, slip-resistant behaviour and demountability of iSRR connectors.

4. Long-term loading experiments

To further quantify connector performance in hybrid steel-FRP bridges, long-term loading experiments were carried out on simplified Single Lap Joint (SLJ) shear specimens. The iSRR connector configuration was altered in this experimental series to enable full preloading of the connector. To facilitate this, the steel coupler and bolts are removed and replaced with a single M20 Grade 10.9 threaded rod. The rod is fastened to the steel plate by means of one and two nuts on the exposed side of the steel plate and within the iSRR injected piece, respectively (as shown in Fig. 5.d). As an alternative to the iSRR connector, a commercially available slip-resistant connector type, namely epoxy Injected Bolts, were investigated. Lastly, Lindapter bolts M20 (grade 8.8), as used in the static push-out experiments, are also tested under long-term loading as readily used connection type where shear load transfer and initial stiffness is not essential, thus no hybrid interaction is accounted between FRP deck and steel structure.

4.1. Experiments

The aforementioned connectors have been tested under three different load regimes: monotonic static loading (see Section 3), fatigue loading and sustained loading (creep). The experimental set-up used in each load testing regime is shown in Fig. 10. The independent connector

slip behaviour of each of the 2 connectors in per specimen was determined by placing a pair of LVDTs on both sides of each connector, as seen in Fig. 10.a). The load applied by the hydraulic jack, and the average connector slip (measured from the 2 LVDTs) were used to construct load-slip curves in the static and fatigue experiments in this experimental campaign.

Based on these monotonic static loading regime results (see Section 3), loading range for both the creep and fatigue experiments was selected. A long-term loading level of 40 kN was selected, which equates to 25–30% of the static shear resistance of the SLJ specimens.

Fig. 11 shows the displacement increases measured per connector for each of the three tested connector types. In Fig. 11, a distinction is made between specimens that were tested under cyclic loading (series F – plotted in red) and specimens tested firstly under sustained loading (creep) and then subsequent cyclic loading (series C – plotted in black). The vertical axis, showing the displacement increase, is limited to the adopted displacement criterion of 0.3 mm.

Fig. 12.a shows the characteristic stiffness degradation vs. load cycles of “slip-resistant” connector types, namely iSRR and Injected Bolt. One results out of six specimens tested per each type are shown. These connectors were loaded by cycles of ± 40 kN until an increase in slip displacement of 0.3 mm was reached. This displacement increase limit was adopted from Annex G of BS EN 1090-2:2008 [18], as defined for slip-resistant connection in steel structures. Such stringent additional slip displacement criterion was not imposed to the blind-bolted “slip type” connectors, namely Lindapter connectors, due to their initial slip behaviour. The criterion used in this case was either bolt fracture or rapid increase of slip due to excessive bearing deformation in FRP plate. iSRR connectors were able to sustain on average 2,000,000 load cycles, whereas Injected Bolts on average sustained 25,000 cycles until additional slip displacement of 0.3 mm, equivalent to approx. 35% of connection stiffness degradation, as shown in Fig. 12.a. This is due to load transfer in iSRR through reinforced injection material possessing higher stiffness than the regular polymeric-only injection material, allowing for larger hole diameters which in turn reduces stress concentrations in facing of FRP panel. None of the slip-resistant connectors suffered fracture of the bolt or injection material due to fatigue loading up to the 0.3 mm additional slip criterion. Lindapter connectors

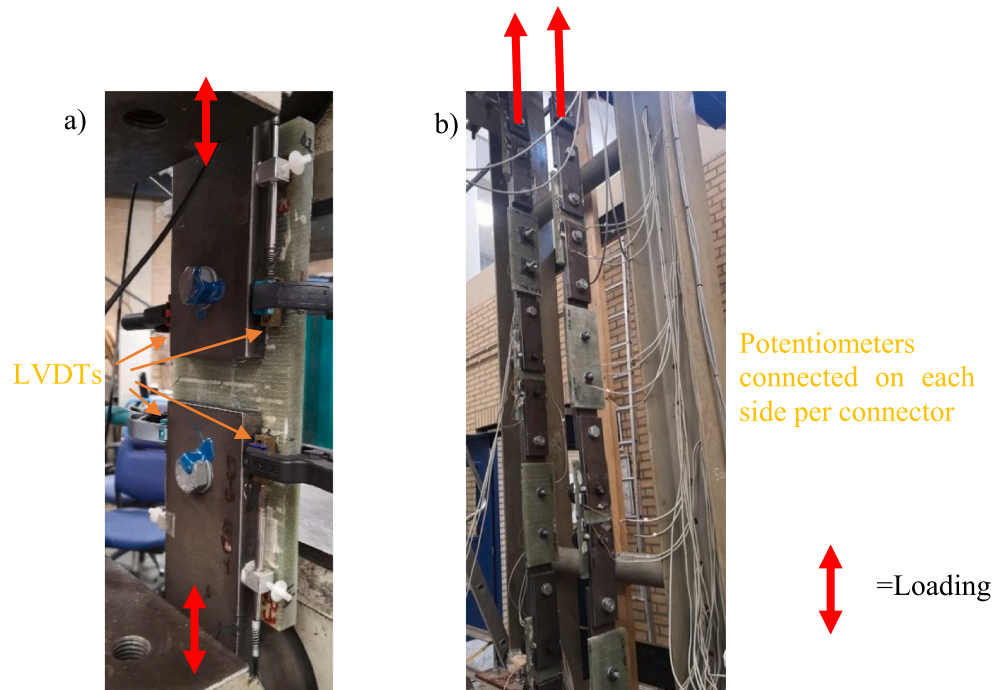


Fig. 10. Experimental set-up. a) Static loading and fatigue loading experiments and b) sustained loading (creep) experiments.

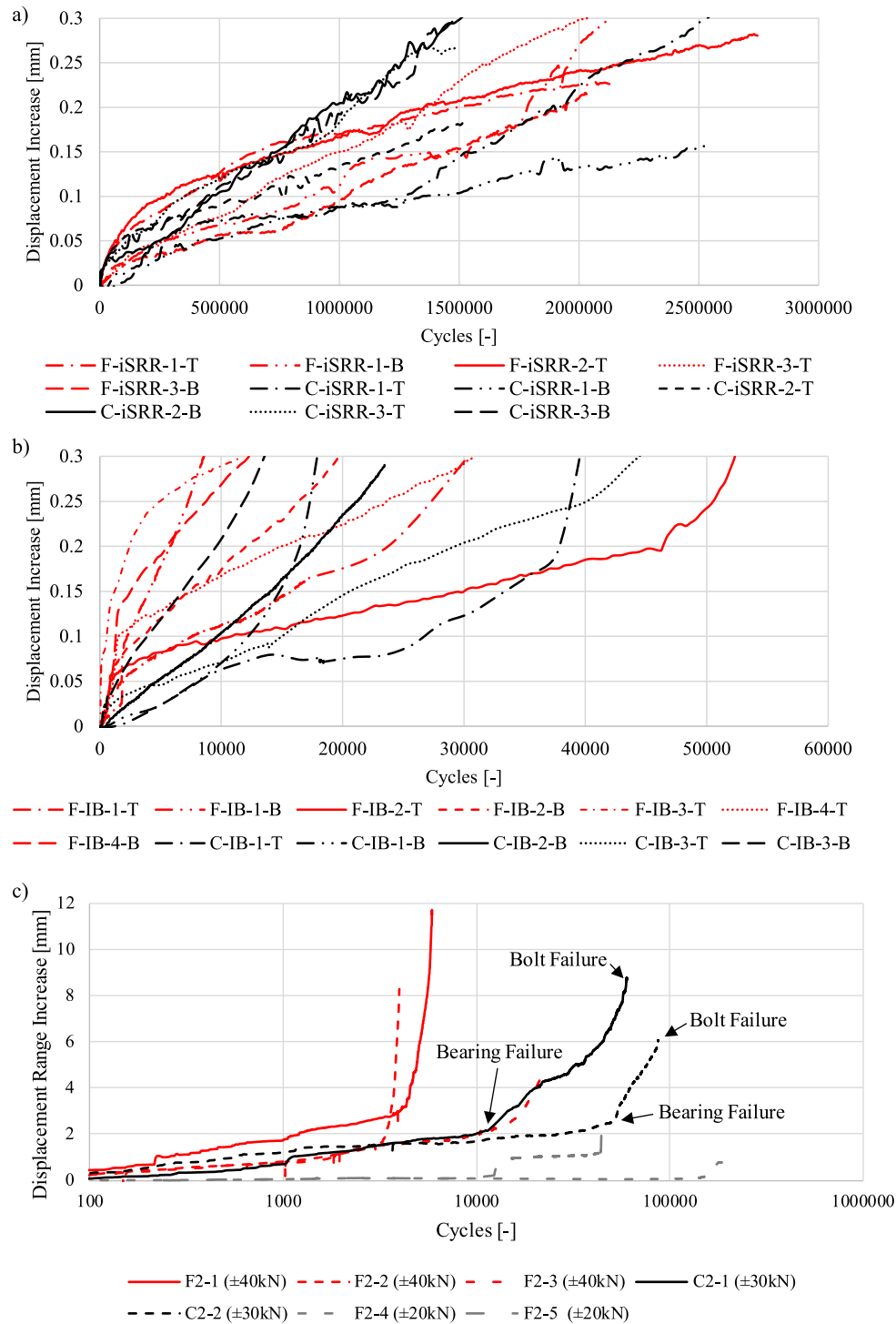


Fig. 11. Displacement range increase vs number of cycles. a) iSRR connectors [9], b) Injected Bolt [9] connectors and c) Lindapter connectors [11].

subjected to the same shear load range ± 40 kN failed by excessive bearing at 8,000 cycles on average, as shown on example results in Fig. 12.b. A twice lower load range on Lindapter connectors resulted in bolt head fracture after 280,000 cycles on average (see Fig. 11). The stiffness of each connector is calculated by the quotient of applied force range vs. displacement range at each load cycle. The relative stiffness is then calculated at each load cycle as normalised to the stiffness obtained in the 1st load cycle. This relative stiffness was used to characterise the connector endurance in fatigue experiments and is shown in Fig. 12 for representative connectors of each of the three connector types.

The average number of cycles to failure per connector type, as

obtained in the experimental campaign on SLJ specimens, is summarised in Table 3.

Creep tests comprised of maintaining a constant 40 kN load. During the two months of sustained 40 kN tensile shear load in a single lap set-up, individual connector displacement was monitored. The initial displacement δ_e resulting from the load application at the start of the experiment was recorded and subtracted from the total measured displacements δ . As such, the creep displacement δ_c resulting from sustained loading only are determined. The results per connector as measured on 3 specimens (each consisting of two connectors labelled top T and bottom B), are shown in Fig. 13.

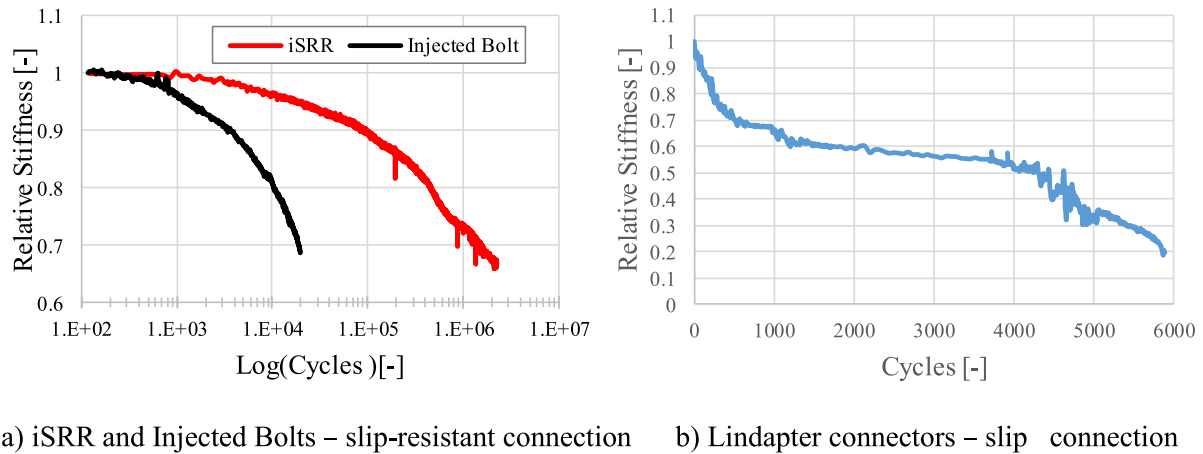


Fig. 12. Shear stiffness degradation of representative connector samples as indication of connector fatigue performance.

Table 3

Average number of cycles to failure - fatigue experiments on SLJ specimens.

Load Range [kN]	SLJ IB	SLJ Lindapter	SLJ iSRR
±20	–	283,248 *	–
±30	–	31,894 **	–
±40	23,730 ***	8,054 **	2,310,000 ***

* - Bolt failure under the head; ** - excessive bearing deformation (>0.3 mm);

*** - increase of slip deformation (>0.3).

After two months of loading, it was found that Lindapter and Injected Bolt connectors on average showed a 50% and 70% higher creep displacement, respectively, as compared to the iSRR specimens (and Table 4).

When considering the effect of prior sustained loading before cyclic loading, it was found that iSRR connectors reached the 0.3 mm criterion under cyclic loading 20% sooner. Due to the low number of achieved cycles as well as scattering of experimental results, no clear influence of prior sustained loading on fatigue performance of Injected Bolts was discernible.

The residual static resistance of SLJ samples of iSRR connectors after subjection to combined long-term loading (64 days sustained 40 kN + 2 million cycles of ±40 kN load) was unchanged compared to the static resistance obtained under short-term loading only. On the other hand,

residual static resistance of Injected Bolts after same long-term loading regime was reduced on average by 30%. This result further illustrates the potential of the iSRR connector to be used in applications where a high fatigue endurance is required [9].

Based on the obtained results, the following application fields are recommended per connector type: the Lindapter connector is to be selected as blind-bolted connector to be used in connection of FRP decks in non-hybrid and non-fatigue applications, such as pedestrian and cyclist bridges. The other two connectors (Injected Bolts and the iSRR connector) are potential candidates for slip-resistant connection in hybrid construction where good fatigue performance is required. Injected Bolts were shown to be less resistant under cyclic loading and display higher creep displacements under sustained loading as compared to the iSRR connector. Furthermore, by enabling full preloading onto steel alone and ensuring service loads are kept below the applied preloading force, the long-term behaviour of iSRR connector is superior.

Table 4

Creep Displacement after 2 months sustained loading.

Connector Type	SLJ IB	SLJ Lindapter	SLJ iSRR
Creep displacement [mm]	0.17	0.15	0.10

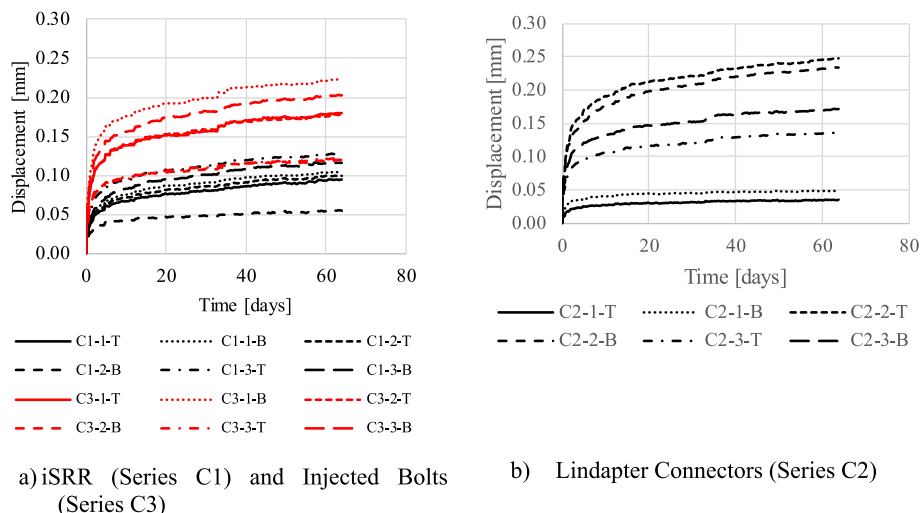
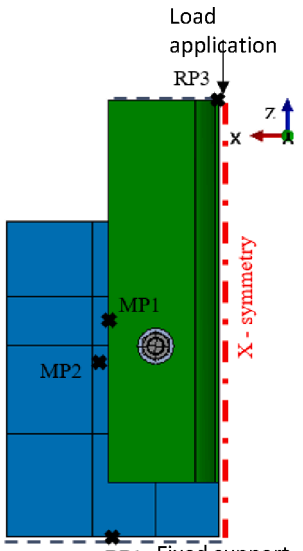
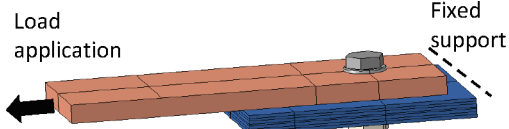
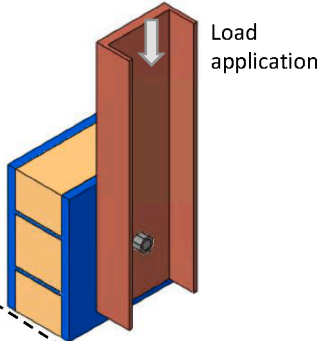


Fig. 13. Creep displacement [9,11].

Table 5
Overview of numerical models reported in this study.

Type of experiment	Type of connector			
	Ajax	Lindapter	iSRR	Injected
 <p>Load application RP3</p> <p>Relative displacement measurement MP1 MP2</p> <p>X - symmetry</p> <p>RP1 Fixed support</p> <p>Push out – Static loading</p>	FEM	FEM	FEM	N/A
 <p>Load application</p> <p>Fixed support</p> <p>SLJ – Static and cyclic loading</p>	N/A	FEM	FEM	FEM
 <p>Load application</p> <p>Fixed support</p> <p>Realistic boundary conditions – Static loading</p>	N/A	N/A	FEM	N/A

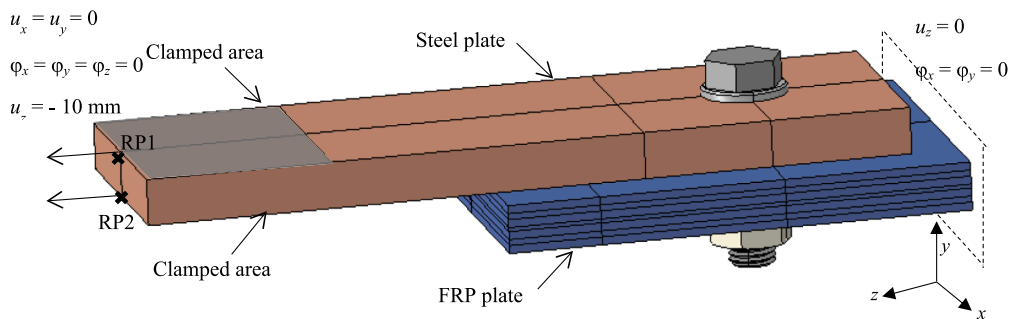


Fig. 14. Boundary conditions of the FE models - example of the SLJ IB set-up.

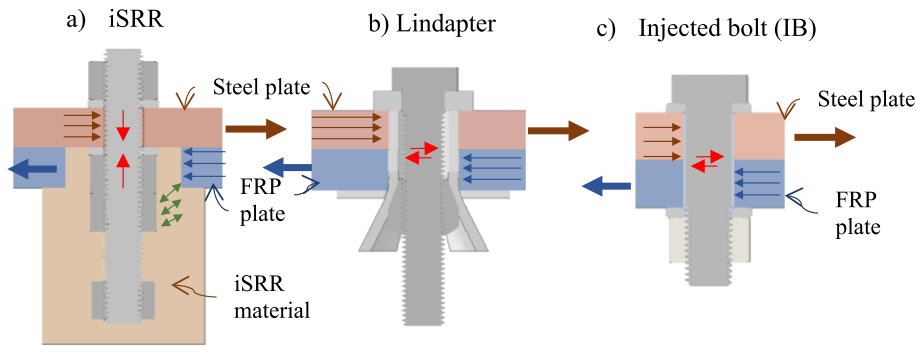


Fig. 15. Geometry and load transfer mechanism of the three connectors in the FE models.

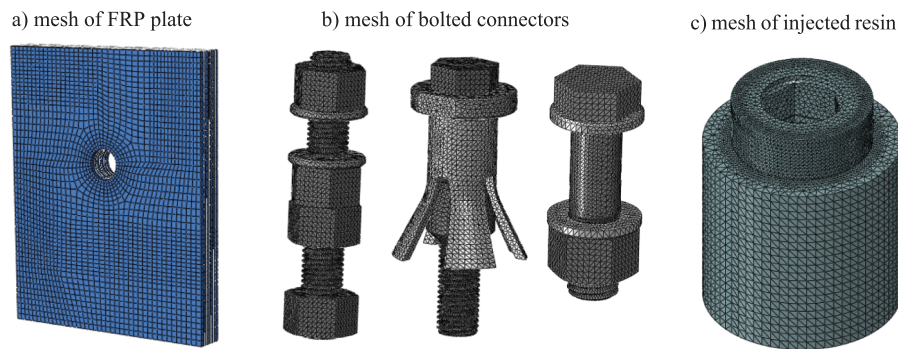


Fig. 16. Details of FE mesh.

5. Numerical studies related to short- and long-term loading experiments

5.1. Description of the model

In this paper 3 types of numerical models were used with the following corresponding goals:

- Models of the push-out experiments: to obtain insightful results with respect to the shear behaviour of the connectors
- Models of the single-lap shear experiments: to explain the findings of the fatigue test results
- Models with different boundary conditions for the fatigue tests: to analyse the consequences of different boundary conditions of the fatigue tests.

The 3 types of numerical models are shown in Table 5.

In this paper the FE models of the single-lap joints and the models with realistic boundary conditions are described in detail.

The single-lap shear FE models were composed of a steel plate, half of the FRP plate and the bolted connectors including injection material, Araldite resin and SRR, in case of injected bolt (IB) and iSRR connection, respectively, see Fig. 14. The bolted connectors were modelled by their exact geometry, including threaded bolts, nuts, washers and sleeve in case of Lindapter connector, as can be seen in Fig. 15. Symmetry boundary conditions were defined at the end surface of the FRP plate. The clamped conditions of the steel plate between the wedges were represented by preventing the translations of the nodes on the surfaces under the wedges. The load was applied as prescribed displacement on the top and bottom clamped surface with a smooth step amplitude curve, to prevent creation of inertia effects.

The bolts, nuts, washers, sleeve and resin materials were built up from linear, four-noded tetrahedron elements C3D4 to follow the difficult geometry of the specimens. Linear, eight-noded solid elements,

Table 6

Contact interaction between different parts of the FE models.

Part instance		Contact type	
1	2	Lindapter model	IB and iSRR models
FRP sub-laminate	FRP sub-laminate	CZM _{FRP}	CZM _{FRP}
Steel plate, sleeve	FRP plate	$\mu = 0.35^*$	$\mu = 0.35^*$
Steel plate	Connectors	$\mu = 0.5$ [19]	$\mu = 0.5$ [19]
Bolt	Nut	$\mu = 0.14$ [20]	$\mu = 0.14$ [20]
Nut/bolt head	Washer/nut/sleeve	$\mu = 0.5$ [19]	$\mu = 0.5$ [19]
Steel parts	SRR	–	CZM _{SRR}
FRP plate	SRR	–	CZM _{SRR}
Steel parts	Araldite resin	–	$\mu = 0.6^*$
FRP plate	Araldite resin	–	$\mu = 0.6^*$

*Obtained through analytical hand calculations to match slip resistance to SLJ test results.

C3D8R with reduced integration and enhanced hourglass control were employed to model the steel plates. 2.5D stacked-shell approach was chosen to model the GFRP composite plate. The laminate was divided into seven sub-laminates through the thickness. The sub-laminates were composed of four-noded SC8R continuum shell elements. Global mesh size of 5 mm was applied in the models, around the shear connectors the mesh was refined: an element size of 1.2 mm for the threaded parts of bolt and coupler, and 2 mm tangential and 3 mm radial mesh in the continuum shell elements of the FRP laminate surrounding the hole (see Fig. 16).

The FE models contain several different interaction surfaces simulated either by the general contact algorithm of Abaqus/Explicit or Cohesive Zone Models (CZM). The contact interaction between different parts of the model is summarised in Table 6 with their respective assumed friction coefficients (μ).

The static single-lap experiments were modelled as quasi-static problem using the dynamic explicit solver of Abaqus. The time period

Table 7

Lay-up of the FRP laminate of the single-lap shear tests and the chosen sub-laminates for modelling.

Lay-up	[90/0/UD ₃ /±45/±45/0/90/UD ₂ /±45/0/90/UD] _s
Sub-laminates	[90/0/0 ₃][45/-45/45/-45/0/90][0 ₂ /45/-45/0/90][0 ₂][0/90/45/-45/0 ₂][0/90/45/-45/45/-45][0 ₃ /0/90]

Table 8

Linear-elastic material properties of UD ply.

Material name	Elastic constants [GPa]	Poisson's ratio
Elastic FRP UD ply V _f = 54%	E ₁ = 41.70, E ₂ = E ₃ = 12.9, G ₁₂ = G ₁₃ = 3.56, G ₂₃ = 3.56	ν ₁₂ = ν ₁₃ = 0.28, ν ₂₃ = 0.4

of 600 s was chosen with 0.005 s desired time increment for integration. The analysis was sped up by employing non-uniform, semi-automatic mass scaling on all elements. This technique was efficiently used by the authors in similar large FE models [10].

The analysis consisted of two loading steps. The preloading of the bolt was executed in the first step employing the 'turn-of-nut method' as is described in [21]. The rod of iSRR connection was preloaded to 171.5 kN axial force, the injected bolt and the Hollow bolt were preloaded to 15 kN axial force. The second step represents the displacement-controlled failure loading with a 10 mm horizontal imposed end displacement.

5.2. Material models

The actual lay-up of the tested laminate given in Table 7 was assigned to the layered continuum shell elements forming the FRP plate. Both non-crimp fabrics (±45 and 0/90) were represented by two half as thick UD plies corresponding to the two orientations. Accordingly, all plies were characterised by the same mechanical properties of the UD ply. The seven stacked sub-laminates composing the FRP plate are indicated by internal parentheses in Table 7.

Hashin damage model was applied for the progressive damage analysis of in-plane ply failure [22]. The material is considered as linear elastic until the failure criteria is reached, followed by linear softening of the stress-strain curve, based on the given value of fracture energy. The transversely isotropic, elastic properties and the static strength values of the UD laminate were directly determined from the UD coupon tests [23] and are presented in Table 8 and Table 9. However, the 4 fracture energies were not measured directly, therefore they were calibrated using the 4 coupon tests of the multidirectional laminate. The calibrated nonlinear input parameters of the composite damage model are shown in Table 9.

Cohesive surface interaction property was applied between the sub-laminates to facilitate interlaminar failure. Bilinear traction-separation law was defined for the constitutive behaviour of the cohesive interface. The default contact enforcement method was assigned, which is based on underlying element stiffness [22]. The interfacial shear strength values of both II and III modes were approximated by the ILSS value of the laminate, while the normal contact strength was estimated as 80% of the shear interfacial strength [24–26]. The normal fracture energy of the interface is assumed to be governed by the normal fracture energy of pure polyester resin [27]. The mode II fracture energy of the E-

Table 9

Nonlinear material parameters of UD ply.

	Longitudinal tensile	Longitudinal compression	Transverse tensile	Transverse compression	Longitudinal shear	Transverse shear
Strength [MPa]	846	486	26	116	73	73
Fracture energy [N/mm]	92	80	0.65	1.045	–	–

glass polyester composite is taken from the experimental results of [28]. The parameters for cohesive surface interaction property are summarised in Table 10. The above-described method for the progressive damage modelling of the FRP material and cohesive interfaces is discussed in great detail in [29].

Progressive damage models for metals available in the material library of Abaqus [22] were used in this study. The undamaged response – i.e. plasticity curve – was composed based on the elastic constants ($E = 210$ GPa, and $\nu = 0.3$) and assumed yield stress – plastic strain curve of isotropic hardening for the steel plate (S355) and sleeve of the Lindapter Bolt (S275). The material and damage model of bolts grade 8.8 and 10.9 were adopted from the research of Pavlović [21], where the ductile and the shear damage parameters were calibrated based on standard tensile coupon tests and bolt shear tests. The overview of the applied material models in the steel part of the FE model is shown in Table 11.

Concrete Damage Plasticity (CDP) model integrated in Abaqus [22] was used for modelling the SRR behaviour, as it allows for confinement effects and different compressive and tensile damage. For the compression strength, Young's modulus and tension strength, mean values of $f_c = 74.3$ MPa, $E = 9.3$ GPa and $f_t = 10.1$ MPa, respectively were determined from previous experiments on cylindrical specimens of SRR [13]. In tension, the material is assumed to be linear elastic until it cracks. The cracking appears when the stress reaches the maximum tensile strength, and afterwards a half sinusoidal softening is defined until $0.2 f_t$ is reached at 0.02 cracking strain. The CDP assumes non-associated potential plastic flow. In this study, Drucker-Prager hyperbolic function was used as flow potential. The plasticity parameters were calculated according to [30].

Due to the lack of actual material testing of Araldite resin, the formulation of its material model was completely based on the research of Xin et al. [31], using a uniaxial material model which combines

Table 10

Parameters of cohesive surface interaction property.

	Normal – mode I	Shear – mode II and III
Contact strength [MPa]	25.8	31
Fracture energy [N/mm]	0.65	2.79

Table 11

Overview of material models of steel parts in FE model.

Part	Plasticity curve	Ductile damage	Shear damage
steel plate, backing plate	S355	included	–
Rod – iSRR con., injected bolt	10.9	included	included
Lindapter bolt	8.8	included	included
Nuts – all connectors	8.8	included	included
Washers – all connectors	10.9	–	–
Sleeve – Lindapter con.	S275	–	–

Table 12

Material parameters for the FE model of Araldite resin based on [31].

Young's Modulus E [GPa]	Poisson's ratio ν [–]	Ultimate Strength σ _u [MPa]	β [°]	K [–]	ψ [°]
5.53	0.315	140.71	12.16	0.92	12.16

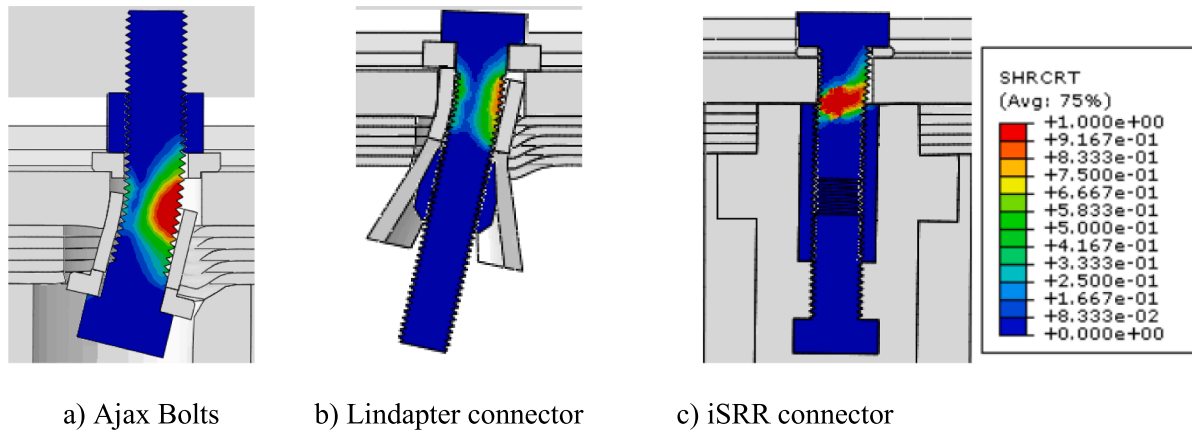


Fig. 17. FEA results of the push-out tests of connectors in FRP deck panels [9].

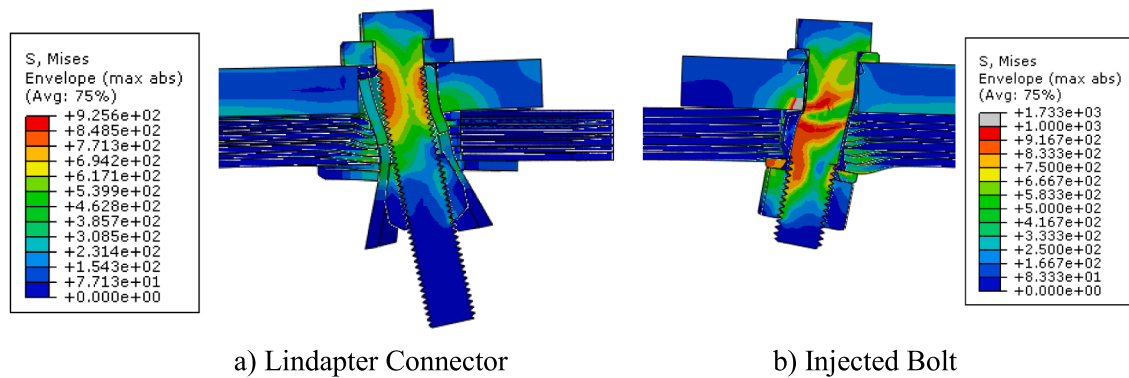


Fig. 18. FEAs of Single Lap Joint tests.

damage mechanics and Ramberg-Osgood relationship to describe the uniaxial compressive behaviour of the resin. The input material parameters (friction angle β , triaxial compression K , dilation angle Ψ) of the Araldite resin used in the FE model is collected in Table 12.

5.3. Load transfer mechanisms from FE results

In the same manner as performed for the single-lap shear experiments, detailed non-linear FE models of push-out tests (modelled in Abaqus) have been created to analyse shear load transfer mechanisms present in the three investigated connectors [10]. Fig. 17 depicts the shear damage index of the steel connectors from push-out FE models at

the load level prior to failure of each connector.

In summary, the blind bolted connectors owe their significant slip capacity and shear resistance to bearing failure of the FRP and catenary effects in the connector. Ajax bolts develop the highest connector axial forces during shear loading, due to effective anchorage by the nut and washer as is illustrated in Fig. 17a. In comparison, FEA demonstrate that Lindapter connectors are not anchored as effectively and subsequently experience bolt rotation which hinder the formation of catenary effects as is shown in Fig. 17b. Finally, load transfer in the iSRR connector was dominated by shearing of the bolt (see Fig. 17c) at the FRP-Steel interface as well as crushing of the injected piece. The connector's ultimate strength and slip is limited by brittle bolt failure.

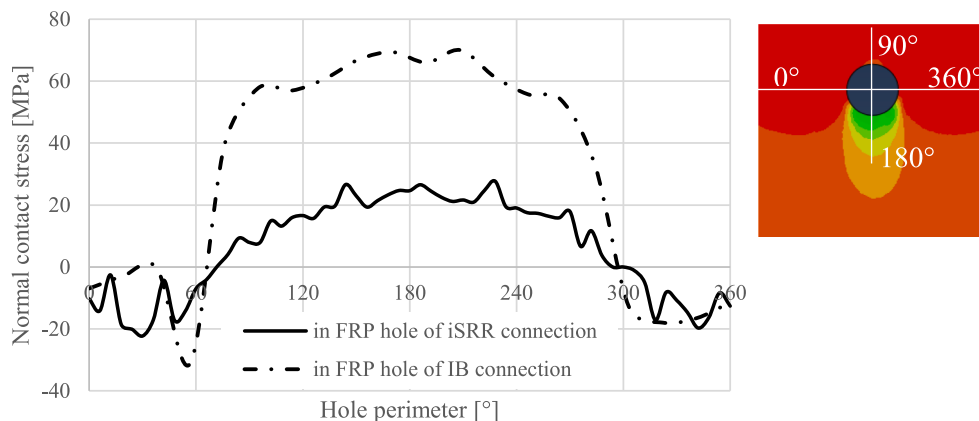


Fig. 19. Bearing (contact) stress in the 1st sub-laminate if FRP plate at 40 kN.

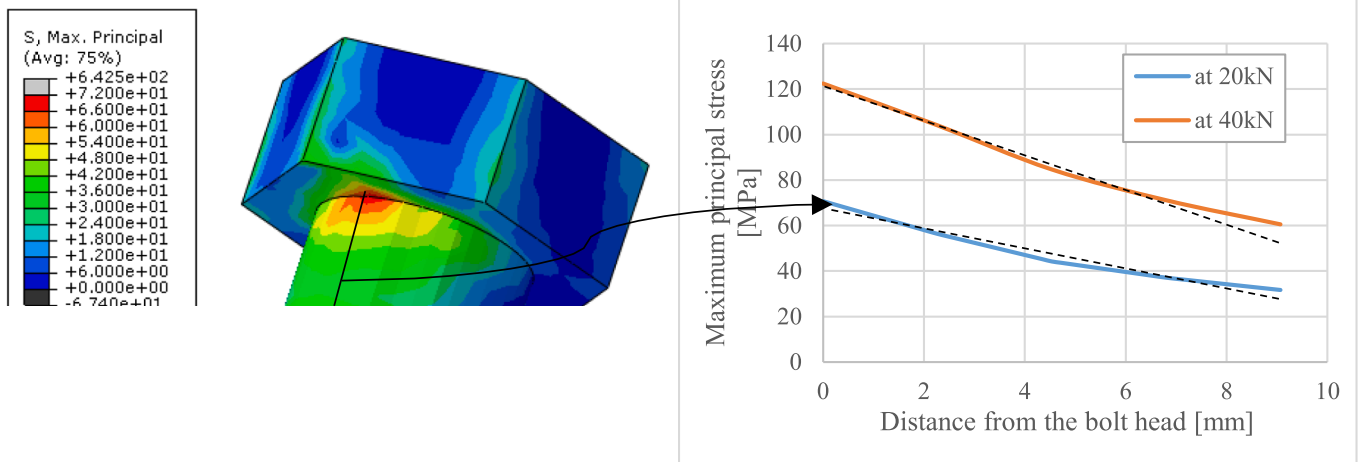


Fig. 20. Stress concentration under the bolt head of Lindapter connector.

Although the development of axial forces has been shown to be beneficial to static shear resistance in blind bolted connectors, it is hypothesised to likely impair fatigue endurance. To verify this statement, specimens in the long-term experimental campaign were analysed in FE analysis (as described in section 5.1) to examine their force transfer mechanisms, see Fig. 18.

The FEAs demonstrate that the iSRR connector engages in force transfer by means of friction via the preloaded threaded rod to steel package, as opposed to shear load transfer in the Injected Bolt and Lindapter connectors. In addition, the iSRR connector experience a minimal loss in axial preload when subjected to the 40 kN shear load level, as applied in the long-term loading experiments. In this load range the iSRR connector relies on force transfer by means of friction, thereby being comparable to the behaviour of a preloaded bolt in steel structures. Injected Bolts and Lindapter bolts are unable to be effectively preloaded due to the presence of FRP within the clamping package, and as such rely on force transfer by means of shear loading of the connector. Under the applied 40 kN shear long-term loading, non-negligible axial forces develop in the Lindapter and Injected Bolt connectors due to catenary effects due to bolt inclination, as shown in Fig. 18.

5.4. Validation and prediction of fatigue life with help of FEA

During fatigue experiments of the non-slip connectors, significantly larger extent of damage (crushing and delamination) was found in the FRP plate of IB connector than that of the iSRR connection, although both non-slip connections were loaded with the same force range of ± 40 kN. Obviously, the magnitude of bearing stress acting on the FRP plate is different in the two connections due to the different hole diameter. The FE models were used to quantify the difference in bearing stress generated in the composite plate due to 40 kN tensile loading of the single-lap shear connection. In Fig. 19, the value of normal contact stress around the perimeter of the hole in the first sub-laminate is plotted. As can be seen, the maximum contact bearing stress in the FRP in case of IB connection is approximately 3 times higher, than the maximum bearing stress that is generated in the FRP plate of the iSRR connection. This leads to nominally 19,000 times more load cycles until equivalent bearing damage in the FRP plate assuming the slope of the S-N curve $m = 9$ (CUR96, [15]). Looking at results presented in Table 3 the possible number of cycles to excessive bearing deformation in the FRP plate of iSRR connectors would be $19,000 \times 23,730$ leading to approximately 450 million cycles. This is much larger than the number of cycles that was obtained until excessive slip deformation due to damage in the SRR piece of these connectors, proving that the design utilising the large diameter of the hole in the FRP plate is effective.

As was stated in Section 4, the Lindapter connector failed by bolt failure under the head of the bolt at the force range of ± 20 kN and by bearing at a force range of ± 40 kN in fatigue testing. With the help of the detailed FE model, an approximate stress concentration factor (SCF) can be determined to characterise the stress at the location of the bolt neck and hence predict the fatigue lifetime of the connector at the two force ranges. The maximum principal stress of the bolt is read from the FE model at 20 kN and 40 kN, see Fig. 20. Due to the steep slope of stress, the dashed line following the trend of the further region is used to determine the stress at the neck.

The stress concentrations and hot-spot stresses of $\sigma_{HSS,20kN} = 63$ MPa and $\sigma_{HSS,40kN} = 121$ MP, in the root of the bolt head for the 20 kN and 40 kN load level, respectively, are obtained from the FE model as shown in Fig. 20. The non-proportionality of the hot-spot stresses vs. the applied load comes from the fact that the connectors are slipping in the hole and rotating at the higher loads, thus releasing some of the stresses in the bolt. Following the recommendations of EN 1993-1-9 [32], assuming the detail class of a non-prestressed bolt in tension loading is ($\Delta\sigma_c = 50$ MPa, $m = 3$), the fatigue life of the connector can be estimated as follows:

$$N = (\Delta\sigma_c / (2 * \sigma_{HSS}))^m * N_c \quad (1)$$

Applying Eq. (1) to results of the FE models leads to $N_{\text{bolt head, } 20kN} = 1.24 * 10^5$ and $N_{\text{bolt head, } 40kN} = 1.8 * 10^4$ number of cycles to bolt failure at the force range of ± 20 kN and 40 kN, respectively.

The experiment shows on average bolt failure at $N = 2.8 * 10^5$ cycles at the cyclic load of ± 20 kN. The numerically determined fatigue life for this failure mode is in the same order of magnitude. The predicted fatigue life is also approx. 2 times conservative which is logical given the fact that numerical prediction is based on characteristic S-N curve from the Eurocode. The fatigue life in cyclic load experiments at ± 40 kN lead to excessive bearing deformation at average $0.8 * 10^4$ cycles. Following the same numerical procedure, the predicted number of cycles required for the bolt failure would be at least 2 times more. This explains the shift in the failure mode from the bolt failure at ± 20 kN to excessive bearing by at ± 40 kN.

5.5. Influence of boundary conditions in fatigue tests

This section aims to verify the influence of the boundary conditions in the fatigue experiments that were previously described. More specifically, these tests were conducted in a SLJ configuration but there is no proof up to now if the set up can be reliable for characterising the fatigue performance of deck-to-girder connections. To further understand this, a more detailed FE model was constructed. This model

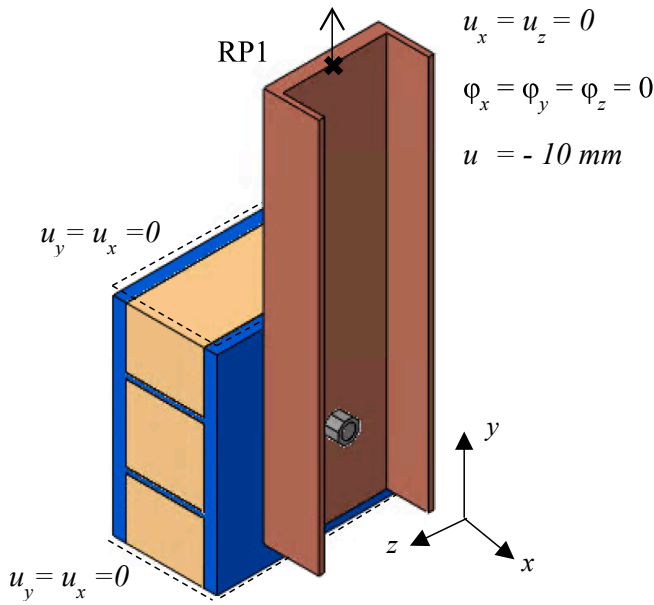


Fig. 21. Set-up of the local FE model mimicking the boundary conditions of the shear connector (iSRR type) in a hybrid beam.

replicates the boundary conditions in the connector that are to be expected in a deck of a hybrid beam. The connector is embedded in a segment of an FRP deck and the steel plate is modelled with flanges to mimic the flexural stiffness of the usual I-Beams in such hybrid structures as shown in Fig. 21. Since the rest of the tests that were tabulated in Table 1 were not conducted under cyclic loading, they were excluded from this comparative study,

Based on the fact that the failure of the injected solution was associated with cracks in the SRR piece, it is reasonable to compare the two set-ups i.e., the single lap configuration with the realistic one, based on the maximum principal stresses that appear inside the SRR piece. The maximum principal stresses are plotted at the applied load of 50 kN and at different path locations, shown in Fig. 22, for both set-ups. One path is located in the direction of the bolt rod, i.e. x-direction, while the other two are placed perpendicular to the bolt rod and to the loading direction, i.e. z-direction. One of the paths in z-direction is located to the surface that is contact with the steel plate and the other one is embedded 3 mm inside the injection piece.

From Fig. 23, it can be concluded that both set-ups have similar magnitudes and trendlines for the maximum principal stresses. The peak values at the edges of the SRR piece that enclose the nuts of the rod are caused due to singularities. To ensure that the results of both set-ups comparable, the geometry of the SRR piece and its mesh size remained identical.

The impact of alternating the boundary conditions is also evaluated

in accordance with the amount of the eccentricity that is generated. This is interpreted by reviewing the flexibility of the two test set-ups and the amount of bending moment that is expected in both cases. As anticipated, the single lap joint geometry is more flexible as it allows for the FRP and steel plated to bend and the SRR piece can freely rotate as shown in the magnified deformed shapes in Fig. 24. However, the amount of bending moment generated in the connector that is comprised by the rod and the SRR piece is identical in both test set ups. This is evident in Fig. 25 where a cut-through of the rod with the injection piece and the nut is made for the same shear force i.e. 41.65 kN at a load level of 50 kN.

6. Conclusions and outlook

FRP offers great potential to reduce weight, maintenance costs and increase lifetime in new built and renovation projects in highway bridges. The current challenge restricting wider application is the lack of knowledge and efficient solutions for slip-resistant connections to FRP in hybrid and knowledge on fatigue and creep behaviour of regular bolted connections in non-hybrid applications. This paper summarises the research conducted into the performance of regular and injected slip-resistant bolted connector types in steel to FRP connections. Two blind-bolted solutions available on the market, Lindapter and Ajax, providing a connection with initial slip are compared to two slip-resistant connector types, the regular injected bolts and novel pre-loaded connectors injected with steel-reinforced resin (iSRR). Results of ultimate load, creep and cyclic (fatigue) connector experiments with different boundary conditions are interpreted with help of detailed Finite Element Models. Following conclusions are drawn:

- 1) iSRR connectors demonstrate the ability to achieve large initial stiffness and shear resistance whilst enabling large execution tolerance and good long term cyclic (fatigue) and sustained load (creep) performance. By changing the connector configuration by increasing the bolt grade, for the same volume of the reinforced resin piece, the connector failure mode is changed from brittle to ductile.
- 2) From the short-term experiments, Ajax connectors offer superior shear resistance due to development of catenary effects, whereas Lindapter bolts offer less shear resistance although ease of installation. The iSRR connector proved to be demountable, possess the highest resistance prior to the onset of non-linearity in pull-out experiments amongst the investigated connectors.
- 3) In the creep experiments, with 2 months sustained load of approx. 25% of the ultimate resistance, the Injected Bolts and Lindapter connectors showed 50% and 70% larger creep deformation compared to iSRR connectors, respectively.
- 4) Slip-resistant joints are required in steel-FRP bridge applications where hybrid interaction between the steel and steel substructure is inevitable and/or desirable. In the long-term cyclic loading experiments in single lap joint configuration, the iSRR connectors

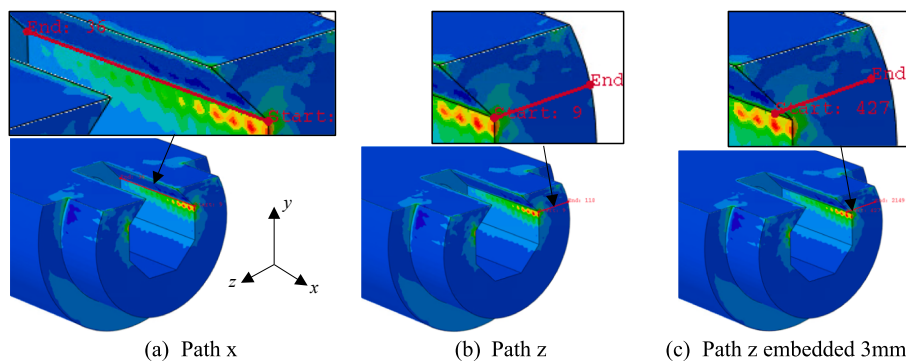


Fig. 22. Paths around the maximum principal stresses.

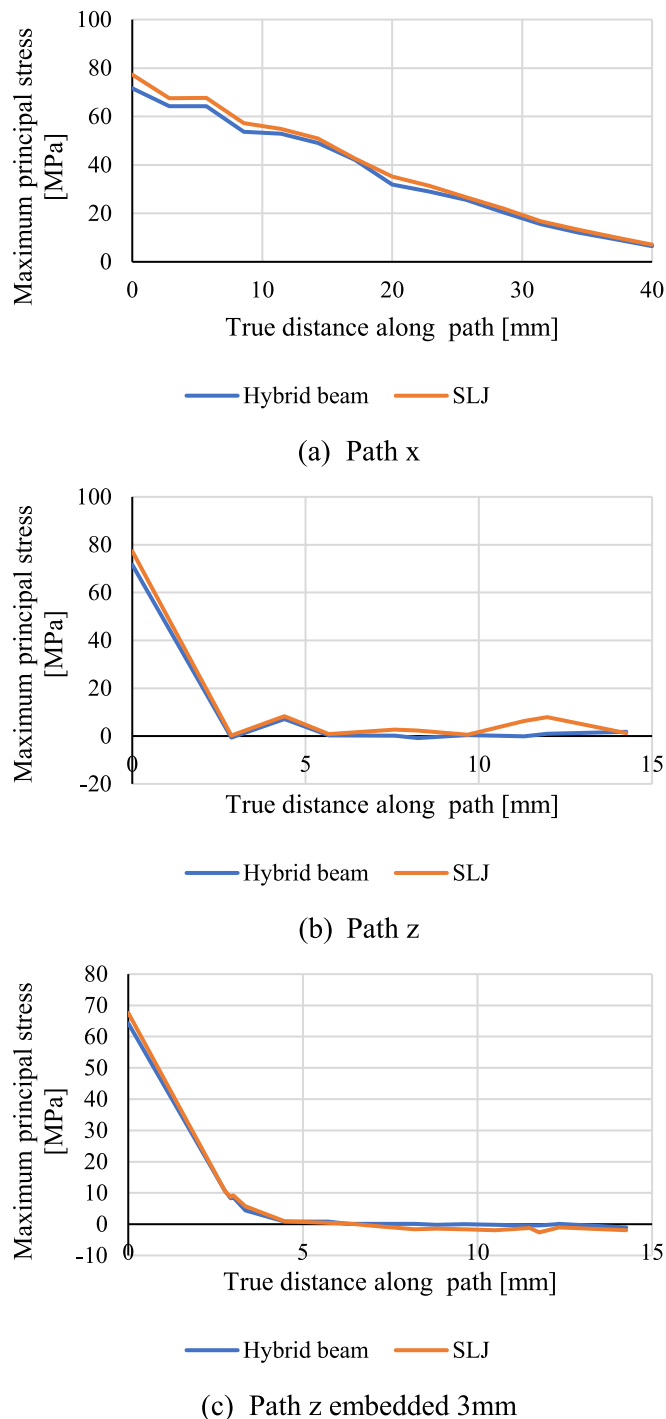


Fig. 23. Influence of boundary conditions on the maximum principal stresses in various path locations.

demonstrated superior fatigue life compared to the Injected Bolts. Approx. 100 times more cycles to the prescribed slip limit of additional 0.3 mm were obtained by iSRR connectors at load range of ± 40 kN corresponding to 25% of the ultimate connector resistance. One of the reasons is that at this load level, the maximum contact bearing stress in the FRP in case the iSRR connection is a third of the stress level in case of the Injected Bolt connection, according to the FE model.

- 5) The SLJ set up is more flexible compared to the set up where the connector is embedded in a segment of a panel. However, the level of bending moment in the connector is identical in both set ups as well

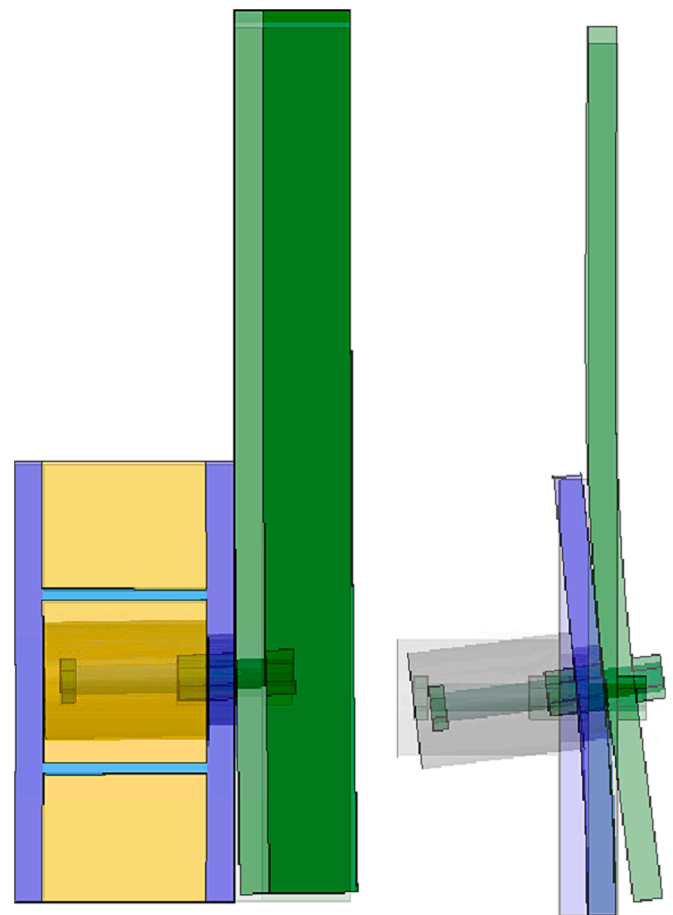


Fig. 24. Deformed shapes magnified by a factor of 10 at 50 kN.

as the hot spot stresses in the SRR piece. From this perspective, SLJ configuration is representative for characterising the fatigue life of iSRR connectors.

- 6) The existing blind-bolted connectors (i.e. Lindapter) demonstrated initial slip behaviour which excludes usage in steel-FRP hybrid structural concepts. However, this does not limit their usage in non-hybrid structures due to their application in a number of existing and future built structures. Relatively short fatigue life is limited by extensive bearing deformation and fracture of the bolt head failure at higher and lower load ranges, respectively. Detailed FE models have been developed to explain the difference in the failure modes at high and low load levels.

CRediT authorship contribution statement

Gerhard Olivier: Methodology, Validation, Data curation, Writing – original draft, Visualization. **Fruzsina Csillag:** Methodology, Validation, Data curation, Writing – original draft, Visualization. **Angeliki Christoforidou:** Methodology, Validation, Data curation, Writing – original draft, Visualization. **Liesbeth Tromp:** Conceptualization, Supervision. **Martijn Velkamp:** Conceptualization, Supervision. **Marko Pavlovic:** Supervision, Methodology, Writing – review & editing, Project administration, Funding acquisition.

Declaration of Competing Interest

The authors declare that they have no known competing financial interests or personal relationships that could have appeared to influence the work reported in this paper.

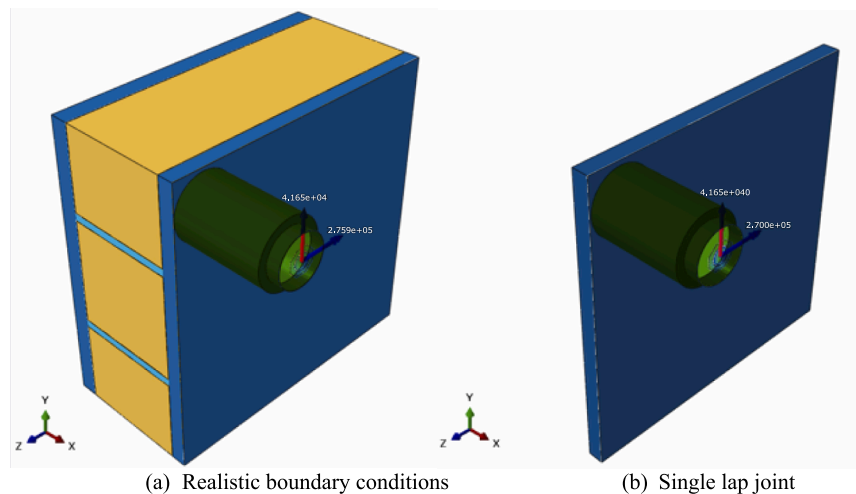


Fig. 25. Influence of boundary conditions on the amount of bending moment at 50 kN, values in N and mm.

Data availability

Data will be made available on request.

References

- [1] T. Keller, H. Gürtler, Design of hybrid bridge girders with adhesively bonded and compositely acting FRP deck, *Compos. Struct.* 74 (2) (2006) 202–212.
- [2] F.L. Moon, D.A. Eckel, J.W. Gillespie, Shear stud connections for the development of composite action between steel girders and fiber-reinforced polymer bridge decks, *J. Struct. Eng.* 128 (6) (2002) 762–770.
- [3] B. Zafari, J. Qureshi, J.T. Mottram, R. Rusev, Static and fatigue performance of resin injected bolts for a slip and fatigue resistant connection in FRP bridge engineering, *Structures* 7 (2016) 71–84, <https://doi.org/10.1016/j.istruc.2016.05.004>.
- [4] C. Wu, Y. Bai, J. Toby Mottram, Effect of Elevated Temperatures on the Mechanical Performance of Pultruded FRP Joints with a Single Ordinary or Blind Bolt, *J. Compos. Constr.* 20 (2016), [https://doi.org/10.1061/\(asce\)cc.1943-5614.0000608](https://doi.org/10.1061/(asce)cc.1943-5614.0000608).
- [5] D.S.E. Abdelkerim, X. Wang, H.A. Ibrahim, Z. Wu, Static and fatigue behavior of pultruded FRP multi-bolted joints with basalt FRP and hybrid steel-FRP bolts, *Compos. Struct.* 220 (2019) 324–337, <https://doi.org/10.1016/j.compstruct.2019.03.085>.
- [6] A.M. Van Wingerde, D.R.V. Van Delft, E.S. Knudsen, Fatigue behaviour of bolted connections in pultruded FRP profiles, *Plast., Rubber Compos.* 32 (2003) 71–76, <https://doi.org/10.1179/146580103225009103>.
- [7] M.P. Nijgh, New Materials for Injected Bolted Connections A Feasibility Study for Demountable Connections, Master's Thesis TU Delft. (2017).
- [8] M.P. Nijgh, A multi-scale approach towards reusable steel-concrete composite floor systems, Doctoral Dissertation, TU Delft, Delft, The Netherlands, 2021.
- [9] G. Olivier, F. Csillag, E. Tromp, M. Pavlović, Conventional vs. reinforced resin injected connectors' behaviour in static, fatigue and creep experiments on slip-resistant steel-FRP joints, *Eng. Struct.* 236 (2021) 112089.
- [10] F. Csillag, M. Pavlović, Push-out behaviour of demountable injected vs. blind-bolted connectors in FRP decks, *Compos. Struct.* 270 (2021) 114043.
- [11] G. Olivier, F. Csillag, E. Tromp, M. Pavlović, Static, fatigue and creep performance of blind-bolted connectors in shear experiments on steel-FRP joints, *Eng. Struct.* 230 (2021) 111713.
- [12] F. Kavoura, A. Christoforidou, M. Pavlovic, M. Veljkovic, Mechanical Properties of Demountable Shear Connectors Under Different Confined Conditions for Reusable Hybrid Decks, *Steel Compos. Struct.* 43 (2022) 419–429. Doi:10.12989/scs.2022.43.4.419.
- [13] F. Csillag, Demountable deck-to-girder connection of FRP- steel hybrid bridges, Delft University of Technology, Delft, The Netherlands, 2018 (Master's Thesis).
- [14] F. Csillag, E. Thie, M. Pavlovic, Tensile and shear resistance of bolted connectors in steel-FRP hybrid beams, in: *Proc. Belgian-Dutch IABSE Young Eng. Colloq.* 2019, YEC 2019, 2019: pp. 50–51.
- [15] CROW, CUR 96: Fibre Reinforced Polymers in Civil Load Bearing Structures, 2017.
- [16] S. Figueira, Injection materials of novel, hybrid steel-reinforced resin joining technology, Hogeschool Rotterdam, 2018.
- [17] EN1994-1-1, Eurocode 4 - Design of composite steel and concrete structures, Part 1-1 Gen. Rules Rules Build. (2010).
- [18] EN 1090-2, Execution of steel structures and aluminium structures – Part 2: Technical requirements for the execution of steel structures, Brussels, Belgium, 2008.
- [19] EN 1993-1-8, Eurocode 3: Design of steel structures - Part 1-8: Design of joints, Brussels, Belgium, 2005.
- [20] ECCS Publication No 38, European Recommendations for Bolted Connections in structural steelwork, Brussels, Belgium, 1985.
- [21] M. Pavlović, Resistance of bolted shear connectors in prefabricated steel-concrete composite decks, University of Belgrade, Belgrade, Serbia, 2013 (Doctoral Dissertation).
- [22] Abaqus-Inc., Abaqus User Manual, Version 6.14., Dassault Systèmes Simulia Corp., USA, 2014.
- [23] L. Cornelissen, Laboratory Report - UD Laminate material tests, TU Delft, Delft, 2019.
- [24] X. Xu, A. Paul, M.R. Wisnom, Thickness effect on Mode I trans-laminar fracture toughness of quasi-isotropic carbon/epoxy laminates, *Compos. Struct.* 210 (2019) 145–151, <https://doi.org/10.1016/j.compstruct.2018.11.045>.
- [25] M. Akterskaia, P.P. Camanho, E. Jansen, A. Artero, R. Rolfes, Progressive delamination analysis through two-way global-local coupling approach preserving energy dissipation for single-mode and mixed-mode loading, *Compos. Struct.* 223 (2019) 110892.
- [26] H. Luo, Y. Yan, T. Zhang, Z. Liang, Progressive failure and experimental study of adhesively bonded composite single-lap joints subjected to axial tensile loads, *J. Adhes. Sci. Technol.* 30 (2016) 894–914, <https://doi.org/10.1080/01694243.2015.1131806>.
- [27] N. Mahmoudi, Effect of volume fiber and crack length on interlaminar fracture properties of glass fiber reinforced polyester composites (GF/PO composites), *Mechanika* 20 (2014) 153–157.
- [28] A. Szekrényes, J. Uj, Mode-II Fracture in E-glass-polyester Composite, *J. Compos. Mater.* 39 (2005) 1747–1768, <https://doi.org/10.1177/0021998305051120>.
- [29] F. Csillag, M. Pavlovic, F. van der Meer, Progressive Damage Analysis of pin bearing failure in GFRP using continuum shell FE modelling approach, *Adv. Compos. Constr.* (2019) 68–74.
- [30] H. Xin, M. Nijgh, M. Veljkovic, Computational homogenization simulation on steel reinforced resin used in the injected bolted connections, *World Congr. Comput. Mech. (WCCM XIII) 2nd Pan Am. Congr. Comput. Mech.* 210 (2019) 942–957.
- [31] H. Xin, M. Nijgh, M. Veljkovic, Computational homogenization simulation on steel reinforced resin used in the injected bolted connections, *Compos. Struct.* 210 (2019) 942–957.
- [32] EN 1993-1-9, Eurocode 3: Design of steel structures – Part 1-9: Fatigue, Brussels, Belgium, 2006.